Keller Box investigation of hybrid nanofluid flow using aluminum alloys over radiative Riga plate surface subjected to variable porous medium

S.R. Mishra[1], MD. Shamshuddin[2*], Subhajit Panda[3], Wubshet Ibrahim[4], Rupa Baithalu[5]

[1]Department of Mathematics, Siksha 'O' Anusandhan Deemed to be University, Bhubaneswar, Odisha-751030, ***India.***

[1]Email: satyaranjan_mshr@yahoo.co.in **ORCID: 0000-0002-3018-394X**

Contact: +91-9937169245

[2]Department of Mathematics, School of Computer Science and Artificial Intelligence, SR University, Warangal-506371, Telangana.* ***India.***

[2]Email: shammaths@gmail.com/md.shamshuddin@sru.edu.in **ORCID: 0000-0002-2453-8492**

Contact: +91-9866826099

[3]Centre for Data Science, Siksha 'O' Anusandhan Deemed to be University, Bhubaneswar, Odisha-751030, ***India.***

[3]Email: spanda.math@gmail.com **ORCID: 0000-0002-4865-0657**

Contact: +91-9861212699

[4]Department of Mathematics, Ambo University, Ambo-14274, ***Ethiopia.***

[4]Email: wubshetib@yahoo.com **ORCID: 0000-0003-2281-8842**

Contact: +251-911892494

[5]Centre for Data Science, Siksha 'O' Anusandhan Deemed to be University, Bhubaneswar, Odisha-751030, ***India.***

[5]Email: rupadhananjaygarnaik@gmail.com **ORCID: 0000-0003-0672-0140**

Contact: +91-9777899400

****Corresponding author Email:*** shammaths@gmail.com

Abstract

The current explores the consequences of radiative heat and the variable porosity on the steady flow of an incompressible hybridised nanomaterial comprising hybrid alloy nanoparticles (AA7072, AA7075) along with water (H_2O) as the conventional fluid. The proposed investigation is performed within the framework of the Riga plate. Because of the complimentary benefits of nanoparticles, hybrid nanofluid is used to improve the efficacy of heat transfer fluids. The flow scenario is characterized by a system of dimensional, nonlinear differential equations renewed to a set of nonlinear dimensionless ordinary differential equations using appropriate similarity substitution. The Keller Box Method (KBM) then solves these transformed equations. Graphs have been used to inspect the effects of changing physical factors on fluid flow, temperature, and other important measurements. This study evaluates the dependability of the results by comparing them to previous research. The results reveal the significant impact of flow

medium inverse porosity influences both the boundary layers to the flow resistance and heat transference characteristics. The Riga plate significantly affects the fluid flow and heat transmission, leading to variations in velocity profiles due to the generated electromagnetic field. Radiant heat influences become more pronounced at higher temperatures, growing heat transport for high-temperature applications.

Keywords: variable porous medium, thermal radiation, hybrid nanofluid, aluminum alloy nanoparticles, Riga plate.

1. Introduction

Hybrid nanofluids are a developed class of nanofluids, which are engineered by suspending hybrid nanoparticles in a host liquid. These innovative liquids combine the developed heat transport properties of traditional nanofluids with the added benefits of synergistic impacts arising from the combination of multiple nanoparticles. The hybrid nanoparticles can be made from various mixtures, such as metal-metal oxide, metal-carbon, or carbon-carbon nanotubes, leading to larger thermal performance, stability, and versatility associated to single-component nanofluids. Huminic et al. [1] considered water-based graphene oxide nanofluid and water-ethylene glycol in 1:1 ration base liquid with silver to carry out the thermal properties of nanofluids under several conditions. Mahboobtosi et al. [2] explored the impact of tri-hybrid nanofluid and compared their results with water-based copper nanofluid. In particular, the trihybrid nanofluid comprised of MoS_2, Cu, and Ag nanoparticles to perform their characteristics over various flow phenomena. The circulation of hybridized nanomaterial around a cylinder, considering the influence of radiating heat for the assumption of Rosseland approximation vis-à-vis the role of activation energy explored by Madhu et al. [3]. Moreover, the present study shows the results obtained using the "shooting technique" and the "Runge-Kutta Fehlberg 45" numerical approach. Imoro et al. [4] scrutinized the magnetohydrodynamics flow of hybridized nanoliquid through thermal radiation in their study assuming blood as base liquid. The governing equations are handled utilizing the "Laplace transform method" associated to modified Bessel functions. Saleem et al. [5] explored an MHD hybrid nanofluid flow including a colloidal mixture with the conventional fluid. A standard numerical approach i.e., the "Keller box method" is used to analyze the proposed model. Hybrid nanofluids have recently gained keen attention for their effective thermal properties widely used in applications like solar water heaters, etc. The hybridized nanomaterial movement via an inclined stretching disk was

investigated by Alharbi et al. [6]. Moreover, the impact of variations in thin film and inclined disc configurations is taken into account. Ali et al. [7] scrutinized the Darcy-Forchheimer model-based flow features of a double-hybridized nanomaterial via a Riga plate and the results are depicted by withdrawing the effect of thermal radiations. The nanofluid comprises two different nanoparticles likely Silicon Graphite (C) and Carbide (SiC) suspended in Ethylene glycol. Additionally, they analyzed the "Cattaneo-Christov heat flux model" within the governing equations.

Thermal radiation generally majors the released electromagnetic radiation from the surface of the substance because of the body temperature. Understanding thermal radiation is crucial in fields such as astronomy, materials science, and engineering, where precise control or utilization of heat transfer processes is necessary. Panda et al. [8] deliberated the control of thermal stratification and radiative heat considering Powell-Eyring non-Newtonian fluid via Riga plate to evaluate the "Cattaneo-Christov heat flux model". Moreover, the inclusion of thermal transport phenomena along with radiant hear significantly enhances the scope of the study. The subsequent nonlinear PDEs are altered into ODEs and solved numerically deploying the "Runge-Kutta method" in connect with a "shooting approach", a reliable numerical technique. Zehra et al. [9] explored the thermal transference phenomena of nanofluid using the "Casson nanofluid model", incorporating the "double diffusional Cattaneo-Christov heat flux model". In their study, the focus was on a curved tube that either shrinks or widens. Concurrently, Salahuddin et al. [10] scrutinized the "Cattaneo-Christov model" in a 2-D stagnation point flow of nanoliquid's, considering activation energy and the viscosity effects in need of temperature. Shoukat et al. [11] applied the theory of "Cattaneo-Christov double diffusion" to investigate Powell-Eyring fluid flowing concluded a convective sensor plate, seeing the role of an applied magnetized field and radiation effects. Awan et al. [12] investigated an Eyring–Powell model for nanofluid flow through a Riga plate surface. Shah et al. [13] explored a numerical model for the Carreau–Yasuda nanofluid upon a Riga plate, incorporating a variable thermal conductivity. Akbar et al. [14] analyzed a Riga plate in motion which was subjected to thermal characteristics employing Tiwari-Das model. Ali et al. [15] discussed the behaviour of H_2O-based Al_2O_3-Cu/ hybrid nanomaterial under the conditions of heat flux and heat dissipation. Ali et al. [16] anticipated the behavior of a H_2O-based Al_2O_3-Cu/ hybrid nanomaterial via a Riga plate under conditions of significant suction and numerical approach i.e., the "Adams-Bashforth technique" is employed to

handle the system. Ali et al [17] studied the impact of Cattaneo-Christov characteristics of hybrid nanofluid. Moreover, the consequences of radiations and joule heating are also considered by introducing wall properties. Mumraiz et al. [18] addressed the heat transport under the application of hybrid nanofluid. This examination portrays the consequences of non-uniform heat flux variations. Furthermore, a detailed analysis is performed to investigate different dimensionless parameters affect the flow fields graphically. Eswaramoorthi et al. [19] analyzed the characteristics of inertial drag for the Darcy–Forchheimer flow model in silver~water nanofluid flowing over Riga plate, considering dissipation and effect of radiation. Hybrid methodology is employed for the revised flow problems through the help of bvp4c presented in MATLAB and the "Homotopy Analysis Method". Kumar et al. [20] scrutinized the thermal assets of radiative third-grade nanomaterial over a sensor plate via a porous medium considering convective conditions. An investigation examines the free convection of a magneto-polar material through an elongating surface considered by Baithalu and Mishra et al. [21] with the diversified role of radiant heat and reacting species. Pattnaik et al. [22] reported a numerical scrutinization of nanomaterial movement past a radially widening sheet, incorporating radiant heat. Moreover, the study presents and discusses the physical behavior of several parameters. A new mathematical model has been created to study the diffusion of reactive species under forced convection of nanofluid by Pattnaik et al. [23]. Additionally, the validation involves implementing an "Adams-Moulton predictor–corrector" numerical scheme. Panda et al. [24] presented the movement of Williamson liquid within two parallel sheets. They also explored the interplay the combined effect of radiation and Joule heating. Furthermore, they applied "*Homotopy perturbation method (HPM)*" to solve the transformed equations analytically. Baithalu and colleagues [25] investigated the flow behavior of a nanoliquid that combines magneto and polar properties on a flexible surface. Moreover, their work explored a couple of stresses and shear rates that significantly influence the flow dynamics. Raju and Sandeep [26] investigated the Casson-Carreau liquids adjacent to a widening surface. Tlau and Ontela [27] focused on the movement of hybrid nanofluids in a porous medium with varying permeability. Finally, their work examines the role of hybrid nanofluid, composed of copper vis-a-vis silver solid particles, moving through permeability of the medium. Khan et al. [28] explored a hybrid nanofluid's dynamic flow and heat transfer characteristic incorporating both SWCNT and MWCNT carbon nanotubes. Hussain and colleagues [29] focused on investigating hybrid

nanofluids composed of engine oil and mineral oil infused with carbon nanotubes (SWCNTs and MWCNTs). These nanofluids were studied in the context of their interaction with a revolving cone within a convectively heated permeable environment. Haider et al. [30] studied a "single-wall carbon nanotube" (SWCNT) nanomaterials and hybrid nanomaterials containing CNTs (SWCNT-MWCNT) across an enlarging sheet. The resulting set of ODEs is then solved via the "Runge–Kutta fourth-order method" combined with the "shooting technique". Madhukesh et al. [31] examined the impact of hybrid nanomaterial comprised of water-based Aluminum alloy through a bent elongating sheet by a non-Fourier heat flux model. Furthermore, the governing PDEs were transformed into ODEs utilizing the appropriate similarity rule. Additionally, the flow phenomena are solved utilizing the "Runge-Kutta-Fehlberg fourth-fifth order (RKF-45)" procedure, implementing the "shooting method". The behavior of numerous factors affecting the flow are presented graphically. Ramesh et al. [32] employed the influence of a temperature-dependent heat generation/sink on the flow of Maxwell nanoliquid on a sensor plate. The model incorporates convective thermal and mass boundary constraints. The "finite difference method", combined with the "Richardson extrapolation technique" is utilized for the solution. Iqbal et al. [33] considered the movement of a Casson liquid via a variable thickness Riga plate. Furthermore, a Riga plate is particularly made up of permanent magnets, aligned array of alternating electrodes over a flat surface. Appropriate transformations are utilized to modeled the problem with the influence of radiant heat and viscous dissipation. Finally, the solution of the set of equations is obtained by using the "Keller Box Scheme" in "MATLAB". On the other hand, a comprehensive review on the hybrid nanofluid experiencing several physical aspects different geometries such as stretching cylinder [34], stretching sheet [35], rotating disk [36], and oscillating plate [37].

Focus point of the study

The literature survey finds various research gaps and this lead to the aim of the proposed investigation to;

- Analyse the insertion of radiant heat and variable porosity on the steady flow of hybrid nanofluid containing alloy nanoparticles i.e., AA7072, AA7075 with water as the host fluid.
- Model the flow problem considering the heat transfer scenario over the Riga plate.

- Transform the basic dimensional, nonlinear differential equations into a set of nonlinear dimensionless ordinary differential equations using appropriate similarity conversion variables.
- Employ Keller Box Method (KBM) for the solution of these transformed equations with the inclusion of diversified factors.
- Validate the current outcome with the previously established output in particular as showing a good correlation.

Novelty of the proposed investigation

The aforesaid description of the research gap and objective lead to prepare the novelty of the study;

- The work introduces the use of water~based alloy nanoparticles for enhanced thermal conductivity and heat transfer performance.
- It examines the combined effects of radiative heat transfer and variable porosity on the flow characteristics of the hybrid nanomaterial over a Riga plate.
- The proposed investigation provides the significant impact of inverse porosity on boundary layer resistance and heat transmission characteristics.
- The influence of the Riga plate on fluid flow and heat transmission emphasizing variations electromagnetic field generated by the plate.
- The detailed comparison with conventional fluids is demonstrated through the hybridization of AA7072 and AA7075 aluminum alloys.

2. Mathematical Formulation

We proposed simultaneous thermal transport via an embedded Riga plate in a porous space, resulting in a steady and incompressible hybrid nanofluid flow. The space is considered variable in order to optimize heat transfer. The hybrid nanofluid is created by injecting nanocomposites composed of single as well as multi-walled CNTs into water. Furthermore, the surface is continuously set stretching/shrinking with wall velocity $u_w(x) = ax$ and isothermal heating with temperature T_w. The 2D flow occurs towards $y \geq 0$ of xy the Cartesian plane, which is depicted through Figure 1.

The vector form of the fundamental equations in component form are:

$$\nabla \cdot V = 0 \tag{1}$$

$$V\cdot\nabla V=\upsilon_{hnf}\nabla^2V+F-\frac{\upsilon_{hnf}}{K(x)}V \tag{2}$$

$$V\cdot\nabla T=\alpha_{hnf}\nabla^2T+\frac{Q}{(\rho Cp)_{hnf}}(T-T_\infty)-\frac{1}{(\rho Cp)_{hnf}}\nabla\cdot q_r \tag{3}$$

Where $V=(u,v)$ is the velocity vector, F indicates for the external force term.

The dimensional form of the fundamental equations used form Navier-Stokes followed from [38]

$$\partial_x u+\partial_y v=0 \tag{4}$$

$$u\partial_x u+v\partial_y u=\upsilon_{hnf}\partial_{yy}u+\frac{\pi j_0 M^*}{8\rho_{hnf}}exp\left(-\frac{\pi}{a_1}y\right)-\frac{\upsilon_{hnf}}{K(x)}u \tag{5}$$

$$u\partial_x T+v\partial_y T=\alpha_{hnf}\partial_{yy}T+\frac{Q}{(\rho Cp)_{hnf}}(T-T_\infty)-\frac{1}{(\rho Cp)_{hnf}}\partial_y q_r \tag{6}$$

$$\left.\begin{aligned}&u=u_w(x)+L\frac{\partial u}{\partial y}=ax+L\frac{\partial u}{\partial y},\quad v=0,\quad T=T_w,\quad aty=0\\&u\to 0,\quad T\to T_\infty,\quad asy\to\infty.\end{aligned}\right\} \tag{7}$$

The variable porous space concept is used from [38]

$$K(x)=\frac{m^2\gamma(x)^3}{\left(1-\gamma(x)^2\right)},\gamma(x)=\gamma_0\left(1+\gamma_1 e^{\frac{x\gamma_2}{m}}\right) \tag{8}$$

while γ_1, γ_2 are the constants with respect to particle diameter, γ_0 suggests the ambient porosity, and m, the particle diameter [27, 39]. The properties of hybrid nanomaterial are displayed in Table 1.

Introducing the similarity variables [20], [38]

$$\eta=y\sqrt{\frac{a}{\upsilon_f}},\theta(\eta)=\frac{T-T_\infty}{T_w-T_\infty},u=axf'(\eta),v=-\sqrt{a\upsilon_f}\,f(\eta). \tag{9}$$

Equations (4)-(7) transform as:

$$A_1f'''(\eta)+f(\eta)f''(\eta)-f'(\eta)^2-A_1\frac{1}{\lambda}\frac{\left[1-\gamma_0\left(1+\gamma_1e^{\frac{-\gamma_2\eta}{\sqrt{\lambda}}}\right)\right]^2}{\left[\gamma_0\left(1+\gamma_1e^{\frac{-\gamma_2\eta}{\sqrt{\lambda}}}\right)\right]^3}f'(\eta)+A_2\alpha e^{(-\beta\eta)}=0 \tag{10}$$

$$\frac{1}{Pr}A_4\left(A_3+\frac{4}{3}Nr\right)\theta''+f(\eta)\theta'(\eta)+A_4\chi\theta(\eta)=0 \tag{11}$$

With following conditions

$$\left.\begin{aligned} &f'(0)=1+\delta f''(0),\ f(0)=0,\theta(0)=1, && as\quad \eta=0\\ &f'(\infty)=0,\theta(\infty)=0 && at\ \eta\to\infty \end{aligned}\right\} \tag{12}$$

Emerging terms in the dimensionless nonlinear system are signified as:

$$\left.\begin{aligned} &\lambda=\frac{am^2}{\upsilon_f},\alpha=\frac{j_0M^*\pi}{8U_w^2\rho_f},\quad \beta=\frac{\pi}{a_1}\sqrt{\frac{\upsilon_f}{\alpha_f}},\ \Pr=\frac{\alpha_f}{\upsilon_f},\ \chi=\frac{Q}{(\rho Cp)_f\,a},\\ &\lambda=\frac{am^2}{\upsilon_f},\alpha=\frac{j_0M^*\pi}{8U_w^2\rho_f},\quad \beta=\frac{\pi}{a_1}\sqrt{\frac{\upsilon_f}{\alpha_f}},\ \Pr=\frac{\alpha_f}{\upsilon_f},\ \chi=\frac{Q}{(\rho Cp)_f\,a}, \end{aligned}\right\} \tag{13}$$

Table 2, extracted from Madhukesh et al. [31], presents the actual thermal and physical aspects of water (base fluid) and AA7072 and AA7075 nanoparticles.

Furthermore, the physical quantities combined with various factors i.e., skin friction coefficient (C_f) and heat transportation rate or Nusselt number (Nu). Implementing Eq. (10), the aforementioned physical quantities are shaped as [32-33]

The Engineering quantities are as follows [19]

$$\left.\begin{aligned} &C_{fx}=\frac{\tau_w}{\rho_f u_w^2},\quad Nu_x=\frac{xq_w}{k_f(T_w-T_\infty)}, \end{aligned}\right\} \tag{14}$$

where,

$$\left.\begin{aligned} &\tau_w=\mu_{hnf}\left(1+\frac{1}{\beta}\right)\left.\frac{\partial u}{\partial y}\right|_{y=0},\\ &q_w=-k_{hnf}\left.\frac{\partial T}{\partial y}-\frac{16\sigma^*T_\infty^3}{3k^*}\frac{\partial T}{\partial y}\right|_{y=0} \end{aligned}\right\} \tag{15}$$

Reduced skin friction and Nusselt number in dimensionless form are

$$\left.\begin{aligned} &\mathrm{Re}_x^{\frac{1}{2}}C_f=\frac{\mu_{hnf}}{\mu_f}f''(0),\\ &\mathrm{Re}_x^{-1/2}Nu=-\left(\frac{k_{hnf}}{k_f}+Nr\right)\theta'(0), \end{aligned}\right\} \tag{16}$$

Where $Re_x=xu_w/v_f$ is the local Reynolds number.

3. Numerical solution

In this study, the nonlinear ODEs (10) - (11) along with boundary constraints (12) were numerically computed by employing "the Keller box method". This method is an unconditionally stable finite difference scheme and possesses the desired accuracy for solving boundary layer problems. The procedure of "Keller box method" is implemented through the following sequences of steps:

Step 1: Transform into a system of first-order ODEs.

A system of coupled nonlinear ordinary equations (10) – (11) are transformed to first order by introducing new independent variables.

Step 2: Finite difference discretization

Algebraic equations are obtained from a system of first-order ODEs using central difference approximation at the midpoint $\left(x^i,\ \eta_{j-\frac{1}{2}} \right)$ for mean average and its derivatives as:

$$()_{j-\frac{1}{2}} = \frac{()_j^i + ()_{j-1}^i}{2}, \quad ()'_{j-\frac{1}{2}} = \frac{()_j^i + ()_{j-1}^i}{h_j} \quad \text{for all involved variables}$$

Step 3: Quasilinearization technique

Algebraic equations are linearized based on Newton's algorithm using $(i+1)^{th}$ iterate for all included variables as follows:

$$()_j^{i+1} = ()_j^i + \delta()_j^i \tag{17}$$

Step 4: Block-tridiagonal elimination scheme

Substituting the above expression (17) and dropping the higher order of δ constitutes a linear tri-diagonal matrix form:

$$[A][\delta] = [r] \tag{18}$$

Where $[A]$ is a block tri-diagonal matrix of order 5×5, and $[\delta] = \left[\delta_1, \delta_2, \delta_3, \ldots, \delta_{j-1}, \delta_J\right]^T$, $[r] = [r_1, r_2, r_3, ..., r_{(j-1)}, r_J]^T$, are unknown vector matrix and constants for $1 \le j \le 5$. Then after, applying the elimination technique to the coefficient matrix A and sweep conditions are used. Finally, the solution is obtained through MATLABR2023a where the step length was chosen as $\eta = 0.01$ and the series of iterations is terminated asymptotically at the maximum condition of 10^{-8}.

4. Code validation

In order to validate the MATLAB code for "Keller Box Method", we have compared the results computed by the developed code with earlier published results of Khan et al. [38] and obtainable in **Table 3.** From the table it is disclosed that the approximate solutions indicate excellent agreement with the previous result obtained by Khan et al. [38].

5. Analysis of results

Figures 1 to 12 show the graphs of velocity and temperature profiles against different physical parameters for which the values of parameters $\eta = 1, \Pr = 0.7,\ \lambda = 0.5, \alpha = 0.1,\ \beta = Nr = \chi = 0.5, \gamma_0 = 0.5, \gamma_1 = \gamma_2 = 0.1, \phi_1 = \phi_2 = 0.01$ are fixed but the value $\eta = 0.1, \lambda = 0.7, \alpha = 0.5,$ are only changed for the temperature profile. Next, Figures 13 to 19 indicate the behaviour of skin friction, Nusselt number, and different physical parameters. Finally, the present result was evaluated with the related literature, as indicated in Table 2.

5.1. Flow field discussion

In Fig. 2, the reaction of the hybridized aluminum alloys "AA7072" and "AA7075" fluid velocity to an increasing porosity (λ) value is displayed. As obtained, the velocity profile is boosted due to the induced internal heating, which discourages viscosity and shear stress. Under the influence of the Riga plate, the medium pore is enhanced to allow free nanoparticle mobility to raise the flow velocity field; thus, high medium permeability is associated with high porosity. The drag and electromagnetic forces are reduced to prompt the interaction and dispersion of nanoparticle thermal properties in the fluid, leading to increasing flow velocity. This effect is applicable in optimizing industrial system designs. Fig. 3 exhibits the influence of increasing values of the electromagnetic actuator (α) on the flow dynamics of the hybridized aluminum alloy nanofluids. The Riga plate stimulates an electromagnetic transverse field, which influences the dynamics of the nanofluid flow rate. The Riga plate device is embedded with electrodes and magnets to create a fluid flow perpendicular to electric and magnetic fields. The nanofluid flow experienced a noteworthy velocity change near the plate because of the electromagnetic force. Thus, the orientation and strength of the applied field are optimized to cause a thinner boundary

layer, which induces flow velocity close to the stretchy surface. This correspondingly encourages convective heat transfer that results in the overall enhancement of the flow velocity field.

Fig. 4 illustrates the impact of the non-dimensional Riga term related to the electrode and magnetic width (β) on the velocity profile. The Lorentz force is prompted to resist the flow, causing a rising value of the term progressive decline in the hybrid nanofluid flow velocity. The electrode and magnet's size and shape strongly affect the nanofluid's electric and magnetic field dispersion. The fluid properties and behaviour are affected; thus, the effects must be carefully studied for efficient specific performance. In Figure 5, the ambient porosity (γ_0) effects on the hybridized AA7072 and AA7075 aluminum alloy nanofluids velocity profile is investigated. The term describes the pores within the AA7072 and AA7075 aluminum alloy material. The flow fundamental properties and dynamics are prompted to boost the velocity profile. A convective thermal distribution is induced, and internal thermal generation is inspired to oppose molecular bonding, thus decreasing the boundary layer viscosity, resulting in a propel flow velocity rate. Fig. 6 examines the velocity slip impact on the flow velocity of the hybrid nanofluid. This phenomenon is associated with the boundary wall and the fluid motion; it happens when the fluid fails to completely adhere to the boundary to create a slip. A significant decrease in the velocity field is observed near the wall, which gradually declines far from the nanofluid stream. Therefore, the complexity between velocity slip and nanoparticle thermal property should be consciously analyzed to optimize the engineering usage. Heat transfer within the system is discouraged and shear stress is propelled to reduce the AA7072 and AA7075 aluminum alloy nanoparticle motion and interaction; such causes an overall decrease in the dynamics of the flow characteristics.

5.2. Thermal field discussion

Fig. 7 shows the response of the hybrid nanofluid thermal distribution to an enhancing inverse porosity term(λ). The term depicts the density of the porous media to the pore; the heat conductivity effectiveness decreases with boosting inverse porosity values. The fluid resistance is boosted with rising inverse porosity due to a denser solid matrix. This is because the typical thermal conductivity of the solid matrix is higher than the aluminum alloy hybrid nanofluid. As such, the system's thermal conductivity is raised to incline heat transfer; this prompted interaction leads to augmented heat diffusion and dissipation, thereby reducing the fluid

temperature profile. Also, the porous medium structure affects the thermal boundary layer to induce solid heat transfer to the fluid, consequently damping the thermal fluid field. Fig. 8 displays the temperature profile for variational incline in the Prandtl numbers. The fluid temperature reduces with increasing Prandtl numbers as given in the plot. The parameter characterizes the momentum boundary layer thickness relative to the temperature boundary layer. As observed, the fluid viscosity is strengthened with heat diffusivity, resulting in a damp ambient thermal diffusion and thicker thermal boundary film; heat transfer governs the fluid heat conduction. The choice of Prandtl number depends on the material considered and the particular applications. Fig. 9 demonstrates the temperature distribution to varying values of thermal radiation (Nr). Radiation is an electromagnetic effect that influences heat transfer dimensions at high temperatures, resulting in a rise in thermal conductivity and distribution of nanoparticles. The hybridized aluminum alloy nanofluid relates with radiation to emit and absorb radiative heat, affecting heat transfer. The thermal conduction of the fluid nanoparticle is efficiently enhanced due to the combined impact of radiation, convection and conduction. The thermal conducting strength of nanoparticles depends on the concentration, size, type and dispersion as applied in cooling systems, heat exchangers, and others. Fig. 10 investigates the impact of volume fraction on the temperature distribution. As plotted, the aluminum alloy hybrid nanofluids temperature field is inspired by the nanoparticle's rising volume fraction or concentration. Fluid thermal conduction is improved to propel heat transfer from the hot area to the more relaxed area, leading to a decreasing fluid thermal gradient and rising nanofluid viscosity. Thus, high viscosity opposes convective heat transport with some areas of the system's high local temperature for higher volume fraction. Meanwhile, the viscosity is lower for small nanoparticle volume fractions to enhance the efficient temperature profile. Fig. 11 shows heat generation's influence on the aluminum alloy hybrid nanoparticle thermal propagation. The fluid internal heating arising from reactant species, an electromagnetic actuator, and electrical resistance directly boosted the temperature of the nanofluid; these heat sources must be effectively managed for system stability and control overheating. Hence, the fluid temperature field is improved due to the propagation of nanoparticles in the hybridized nanofluid. The based fluid thermal conductivity is highly improved to support adequate thermal dissipation and lower viscosity for effective heat convection transport. Therefore, heat generation internally needs an appropriate convective mechanism to guarantee uniform temperature distribution and avoid localized

hotspots. Hence, continuous nanoparticle propagation is encouraged to maintain thermal stability despite the thermal source, which requires surfactant for suspension stability.

5.3. Engineering quantities discussion

Figs. 12 to 16 describe the impact of parameter variation on the engineering quantities, specifically the wall friction and thermal gradient. In Figs. 12 to 14, with an asymptotic increase in the velocity slip (δ), a rising value of Hartmann number (α), inverse porosity (λ), and electrode and magnet width (β) are studied on the skin friction. In Fig. 12, enhancing the values of the parameter (α) raises the wall friction of the conducting fluid significantly due to magnetic field influence. The velocity gradient is boosted as the internal heating suppresses Lorentz's force strength to cause a reduction in skin friction. Thus, the aluminium alloy nanoparticles' viscosity, thermal conductivity, and thermophysical properties are altered to influence the boundary layer film, thereby raising the fluid skin friction. Likewise, in Fig. 13, inclining the values of inverse porosity (λ) resulted in rising skin friction. The term depicts porous media with increasing solid matrix density within the medium, which resulted in fluid flow resistance and a high-pressure drop. Therefore, a significant flow restriction is provided, prompting enhanced skin friction. Meanwhile, in Fig. 14, the impact of electrode and magnet width (β) on the skin friction is delivered. As noticed, the skin friction reduces due to the boundary film thinner, which stimulates free fluid flow, which affects the velocity field near the plate surface; the velocity gradient declines to influence the skin friction directly. The term impacted the Lorentz force magnitude for an unvaried velocity field, potentially decreasing skin friction. The induced electromagnetic force optimizes the thinner boundary layer to discourage velocity gradient, thereby reducing skin friction. In Figs. 15 and 16, with asymptotically rising heat generation (χ), the increasing values of the inverse porosity (λ) and thermal radiation (Nr). raises the Nusselt number profiles. The wall thermal gradient of the aluminium alloy hybrid nanofluids increases for both parameters due to inspired heat source terms, thermal conductivity and convective heat distribution. The porosity and radiation terms affected the thermal film viscosity to influence the heat transport coefficient that, in turn, propels temperature gradient with the nanofluid at the surface, thus enhancing the Nusselt number profile.

6. Conclusion

The investigation of heat transport in hybridized AA7072 and AA7075 aluminum alloy nanomaterial-based radiative nanomaterial flow via a Riga plate embedded in a variable porous medium is carried out. The Keller Box technique solves the invariant dimensionless coupled derivative boundary value model. Thus, the study's aim and objectives are achieved. The analysis discloses several vital understandings of the thermal and fluid dynamics behaviour of the systems:

- The hybridization of AA7072 and AA7075 aluminum alloys in the nanofluid significantly enhances thermal conductivity, resulting in improved heat transfer rates compared to conventional fluids.
- Radiative effects become more pronounced at higher temperatures, increasing heat transport for high-temperature applications.
- The presence of flow medium inverse porosity influences both the momentum and thermal boundary layers to alter the flow resistance and heat transfer characteristics,
- The electromagnetic field generated by the Riga plate significantly affects the fluid flow and heat transfer, leading to variations in velocity profiles and thermal gradients.
- The combined effects of the hybrid nanomaterials, radiative heat transfer, porous medium, and electromagnetic field result in complex interactions affecting skin friction and the heat transfer coefficient.

The findings from this study have significant implications for the design and optimization of cooling and heating systems in advanced engineering applications. Combining hybridized nanofluids with magnetic fields and porous media leads to highly efficient thermal management solutions. Future studies can explore optimization techniques to identify the best combinations of nanoparticle concentrations, magnetic field strengths, and porous medium configurations for thermal stability and applications.

Nomenclature

$u \& v$	Components of the velocity	γ_1, γ_2	Empirical constant
λ	porosity parameter	m	Particle diameter
χ	heat generation parameter	γ_0	Ambient porosity
α	Hartmann number	Nu	Nusselt number
Pr	Prandtl number	C_f	skin friction coefficient
δ	velocity slip	m	particle diameter

β	non-dimensional Riga term related to the electrode and magnetic width
Nr	thermal radiation
ϕ	nanoparticle volume fraction

References

1. Huminic, G., Vărdaru, A., Huminic, A. et al. "Broadband absorption and photo-thermal conversion characteristics of rGO-Ag hybrid nanofluids", *J. Mol. Liq.*, **408**, p. 125347 (2024). https://doi.org/10.1016/j.molliq.2024.125347
2. Mahboobtosi, M., Hosseinzadeh, K. and Ganji, D.D. "Investigating the Convective Flow of Ternary Hybrid Nanofluids and Single Nanofluids around a Stretched Cylinder: Parameter Analysis and Performance Enhancement", *Int. J. Thermofluids.*, **23**, p. 100752 (2024). https://doi.org/10.1016/j.ijft.2024.100752
3. Madhu, J., Madhukesh, J.K., Sarris, I. et al. "Influence of quadratic thermal radiation and activation energy impacts over oblique stagnation point hybrid nanofluid flow across a cylinder", *Case Stud. Therm. Eng.*, **60**, p. 104624 (2024). https://doi.org/10.1016/j.csite.2024.104624
4. Imoro, I., Etwire, C.J. and Musah, R. "MHD flow of blood-based hybrid nanofluid through a stenosed artery with thermal radiation effect", *Case Stud. Therm. Eng.*, **59**, p. 104418 (2024). https://doi.org/10.1016/j.csite.2024.104418
5. Saleem, S., Ahmad, B., Naseem, A. et al. "Mono and hybrid nanofluid analysis over shrinking surface with thermal radiation: a numerical approach", *Case Stud. Therm. Eng.*, **54**, p. 104023 (2024). https://doi.org/10.1016/j.csite.2024.104023
6. Alharbi, A.F., Alhawiti, M., Usman, M. et al. "Enhancement of heat transfer in thin-film flow of a hybrid nanofluid over an inclined rotating disk subject to thermal radiation and viscous dissipation", *Int. J. Heat and Fluid Flow.*, **107**, p. 109360 (2024). https://doi.org/10.1016/j.ijheatfluidflow.2024.109360
7. Ali, A., Aslam, M.N., Junaid, M.S. et al. "Thermal analysis in Darcy-Forchheimer hybrid nanofluid through a Riga plate: An ANN optimization", *Case Stud. Therm. Eng.*, **60**, p. 104696 (2024). https://doi.org/10.1016/j.csite.2024.104696
8. Panda, S., Ontela, S., Pattnaik, P.K. et al. "Radiating heat effect on Powell–Eyring blood-based hybrid nanofluid over a Riga plate with thermal stratification Cattaneo–Christov heat flux model", *Part. Diff. Equn. Appl. Math.*, **11**, p. 100769 (2024).

https://doi.org/10.1016/j.padiff.2024.100769

9. Zehra, I., Abbas, N., Amjad, M. et al. "Casson nanoliquid flow with Cattaneo-Christov flux analysis over a curved stretching/shrinking channel". *Case Stud. Therm. Eng.*, **27**, p. 101146 (2021). https://doi.org/10.1016/j.csite.2024.101146
10. Salahuddin, T., Awais, M., Khan, M. et al. "Analysis of transport phenomenon in cross fluid using Cattaneo-Christov theory for heat and mass fluxes with variable viscosity", *Int. Commun. Heat Mass Transf.*, **129**, p. 105664 (2021). https://doi.org/10.1016/j.icheatmasstransfer. 2021.105664
11. Shoukat, Z., Zubair, M.H., Farman, M. et al. "Impacts of joule heating with Cattaneo-Christov heat flux model in a MHD flow of Eyring-Powell fluid on a Riga plate", *Alex. Eng. J.*, **64**, pp. 741-748 (2023). https://doi.org/10.1016/j.aej.2022.10.0067
12. Awan, A.U., Shah, A.A.A., Qayyum, S. et al. "Mixed convected synchronization of gyrotactic microorganism flow of an Eyring–Powell nanofluid over a Riga plate", *J. Appl. Math. Mech.*, **104**(12), p. e202301055 (2024). https://doi.org/10.1002/zamm.202301055.
13. Shah, S.A.A., Qayyum, S., Nadeem, S. et al. "Thermal characterization of Sutterby nanofluid flow under Riga plate: Tiwari and Das model", *Mod. Phys. Lett. B.*, **39**(3), p. 2450421 (2025). https://doi.org/10.1142/S0217984924504219
14. Akbar, A.A., Awan, A.U., Nadeem, S. et al. "Heat transfer analysis of Carreau–Yasuda nanofluid flow with variable thermal conductivity and quadratic convection", *J. Comput. Des. Eng.*, **11**(1), pp. 99-109 (2024). https://doi.org/10.1093/jcde/qwae009
15. Ali, A., Noreen, A., Saleem, S. et al. "Heat transfer analysis of Cu–Al_2O_3 hybrid nanofluid with heat flux and viscous dissipation", *J. Therm. Anal. Calorim.*, **143**, pp. 2367–2377 (2021). https://doi.org/10.1007/s10973-020-09910-6
16. Ali, A., Ahmed, M., Ahmad, A. et al. "Enhanced heat transfer analysis of hybrid nanofluid over a Riga plate: incorporating Lorentz forces and entropy generation", *Tribol. Int.*, **188**, p. 108844 (2023). https://doi.org/10.1016/j.triboint.2023.108844
17. Ali, A., Khatoon, R., Ashraf, M. et al. "Cattaneo–Christov heat flux on MHD flow of hybrid nanofluid across stretched cylinder with radiations and Joule heating effects", *Waves Rand. Comp. Med.*, pp. 1–18 (2022). https://doi.org/10.1080/17455030.2022.2145524

18. Mumraiz, S., Ali, A., Awais. et al. "Entropy generation in electrical magnetohydrodynamic flow of Al_2O_3–Cu/H_2O hybrid nanofluid with non-uniform heat flux", *J. Therm. Anal. Calorim.*, **143**, pp. 2135–2148 (2021). https://doi.org/10.1007/s10973-020-09603-0
19. Eswaramoorthi, S., Divya, S., Goel, R. et al. "Analytical and numerical study of water-based silver nanofluid (Ag) across a Riga plate with nonlinear radiation and viscous dissipation: A three-dimensional study", *Part. Diff. Equn. Appl. Math.*, **10**, p. 100707 (2024). https://doi.org/10.1016/j.padiff.2024.100707
20. Kumar, M., Kaswan, P., Kumari, M. et al. "Cattano Christov double diffusion model for third grade nanofluid flow over a stretching Riga plate with entropy generation analysis", *Heliyon.*, **10**(10), p. e30188(2024). https://doi.org/10.1016/j.heliyon.2024.e30188
21. Baithalu, R. and Mishra, S.R. "On the free convection of magneto-micropolar fluid in association with thermal radiation and chemical reaction and optimized heat transfer rate using response surface methodology", *Mod. Phys. Lett B.*, **37**(33), p. 2350171(2023). https://doi.org/10.1142/S0217984923501713
22. Pattnaik, P.K., Pattnaik, J.R., Mishra, S.R. et al. "Variation of the shape of Fe_3O_4-nanoparticles on the heat transfer phenomenon with the inclusion of thermal radiation", *J. Therm. Anal. Calorim.*, 147, pp. 2537–2548 (2022). https://doi.org/10.1007/s10973-021-10605-9
23. Pattnaik, P.K., Mishra, S.R., Bég, O.A. et al. "Axisymmetric radiative titanium dioxide magnetic nanofluid flow on a stretching cylinder with homogeneous/heterogeneous reactions in Darcy-Forchheimer porous media: Intelligent nanocoating simulation", *Mat. Sci. Eng: B.*, **277**, p. 115589 (2022). https://doi.org/10.1016/j.mseb.2021.115589
24. Panda, S., Pradhan, G., Nayak, D. et al. "Presentation of entropy due to heat transfer irreversibility of MHD Williamson fluid over an inclined channel", *Mod. Phys. Lett B.*, **38**(7), p. 2450010 (2023). https://doi.org/10.1142/S0217984924500106
25. Baithalu, R., Mishra, S.R., Pattnaik, P.K. et al. "Optimizing shear and couple stress analysis for the magneto-micropolar dissipative nanofluid flow toward an elongating surface: A comprehensive RSM-ANOVA investigation", *J. Therm. Anal. Calorim.*, **149**, pp. 1697-1713 (2023). https://doi.org/10.1007/s10973-023-12741-w
26. Raju, C.S.K. and Sandeep, N. "Unsteady three-dimensional flow of Casson–Carreau fluids past a stretching surface", *Alex. Eng. J.*, **55**(2), pp. 1115–1126 (2016).

https://doi.org/10.1016/j.aej.2016.03.023

27. Tlau, L. and Ontela, S. "Entropy analysis of hybrid nanofluid flow in a porous medium with variable permeability considering isothermal/iso-flux conditions", *Chin. J. Phys.*, **80**, pp. 239–252 (2022). https://doi.org/10. 1016/j.cjph.2022.10.001
28. Khan, U., Ishak, A. and Zaib, A. "Hybrid nanofluid flow containing single-wall and multi-wall CNTs induced by a slender stretchable sheet", *Chin. J. Phys.*, **74**, pp. 350–364 (2021). https://doi.org/10.1016/j.cjph. 2021.10.009
29. Hussain, A., Haider, Q., Rehman, A. et al. "A thermal conductivity model for hybrid heat and mass transfer investigation of single and multi-wall carbon nano-tubes flow induced by a spinning body", *Case Stud. Therm. Eng.*, **28**, p. 101449 (2021). https://doi.org/10.1016/j.csite.2021.101449
30. Haider, S.M.A., Ali, B., Wang, Q. et al. "Rotating flow and heat transfer of single-wall carbon nanotube and multi-wall carbon nanotube hybrid nanofluid with base fluid water over a stretching sheet", *Energies.*, **15**(16), p. 6060 (2022). https://doi.org/10.3390/en15166060
31. Madhukesh, J.K., Kumar, R.N., Gowda, R.J.P. et al. "Numerical simulation of AA7072-AA7075/water-based hybrid nanofluid flow over a curved stretching sheet with Newtonian heating: A non-Fourier heat flux model approach", *J. Mol. Liq.*, **335**, p. 116103 (2021). https://doi.org/10.1016/j.molliq.2021.116103
32. Ramesh, G.K., Roopa, G.S., Gireesha, B.J. et al. "An electro-magneto-hydrodynamic flow Maxwell nanoliquid past a Riga plate: a numerical study", *J. Braz. Soc. Mech. Sci. Eng.*, **39**(11), pp. 4547–4554 (2017). https://doi.org/10.1007/s40430-017-0900-z
33. Iqbal, Z., Azhar, E., Mehmood, Z. et al. "Unique outcomes of internal heat generation and thermal deposition on viscous dissipative transport of viscoplastic fluid over a Riga-plate", *Commun. Theor. Phys.*, **69**(1), p. 68 (2018). https://doi.org/10.1088/0253-6102/69/1/68
34. Ali, A., Kanwal, T., Awais, M. et al. "Impact of thermal radiation and non-uniform heat flux on MHD hybrid nanofluid along a stretching cylinder", *Sci. Rep.*, **11**, p. 20262 (2021). https://doi.org/10.1038/s41598-021-99800-0
35. Shamshuddin, MD., Pnada, S., Salawu, S.O. et al. "Analysis of Casson ternary nanofluid integration under various thermal physical impacts with Cattaneo-Christov model:

Exploring magnified heat transfer in stretchy surface", *Int. J. Hydrogen Energy.* **101**, pp. 450-460 (2025). https://doi.org/10.1016/j,ijhydene.2024.12.426

36. Hussain, S., Ali, A., Rasheed, K. et al. "Application of response surface methodology to optimize MHD nanofluid flow over a rotating disk with thermal radiation and Joule heating", *Case Stud. Therm. Eng.*, **52**, p. 103715 (2023). https://doi.org/10.1016/j.csite.2023.103715
37. Prabhakar Reddy, B., Shamshuddin, MD., Salawu, S.O. et al. "Computational analysis of transient thermal diffusion and propagation of chemically reactive magneto-nanofluid, Brinkman-type flow past an oscillating absorbent plate", *Part. Diff. Equn. Appl. Math.*, **11**, p. 100761 (2024). https://doi.org/10.1016/j.padiff.2024.100761
38. Khan, A.S., Gul, T., Muhammad, T. et al. "Hybrid nanofluids flow over a Riga plate surrounded by a variable porous medium for heat transfer optimization", *Numer. Heat Transf Part A: Applic.* (2024). (In-press). https://doi.org/10.1080/10407782.2024.2345856
39. Tijani, Y.O., Akolade, M.T. and Kasim, A.R.M. "Transport features on bidirectional nanofluid flow with convective heating and variable Darcy Regime", *J. Comput. Theoret. Trans.*, **52**(5), pp. 343-362 (2023). https://doi.org/10.10180/23324309.2023.2257394

Figure Captions

Fig 1. Diagrammatic representation of the hybrid nanofluid over Riga surface
Fig 2. $f'(\eta)$ Profile for different values of λ
Fig. 3. $f'(\eta)$ Profile for different values of α
Fig. 4. $f'(\eta)$ Profile for different values of β
Fig. 5. $f'(\eta)$ Profile for different values of γ_0
Fig. 6. $f'(\eta)$ Profile for different values of δ
Fig. 7. $\theta(\eta)$ Profile for different values of λ
Fig. 8. $\theta(\eta)$ Profile for different values of Pr
Fig. 9. $\theta(\eta)$ Profile for different values of Nr
Fig. 10. $\theta(\eta)$ Profile for different values of ϕ
Fig. 11. $\theta(\eta)$ Profile for different values of χ
Fig. 12. $\mathrm{Re}_x^{1/2} C_f$ variations with δ for different values of α
Fig. 13. $\mathrm{Re}_x^{1/2} C_f$ variations with δ for different values of λ
Fig. 14. $\mathrm{Re}_x^{1/2} C_f$ variations with δ for different values of β
Fig. 15. $\mathrm{Re}_x^{-1/2} Nu_x$ variations with χ for different values of λ

Fig. 16. $\mathrm{Re}_x^{-1/2} Nu_x$ variations with χ for different values of Nr

Table Captions

Table 1. The thermal relations for hybrid nanomaterials [28-29]
Table 2. Thermal features of the base and nanoparticles
Table 3. Comparison of present result for varied values of α and χ

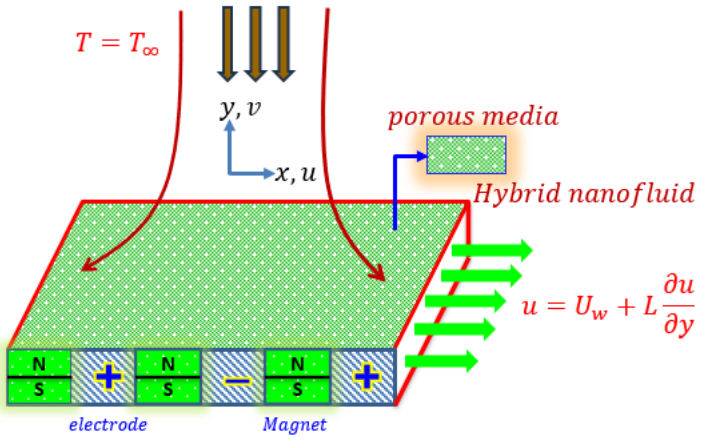

Fig 1. Diagrammatic representation of the hybrid nanofluid over Riga surface

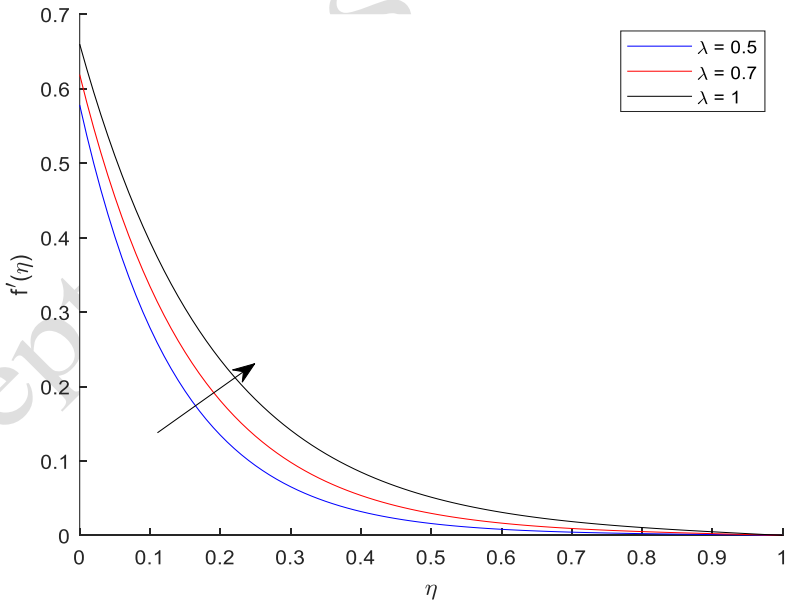

Fig 2. $f'(\eta)$ Profile for different values of λ

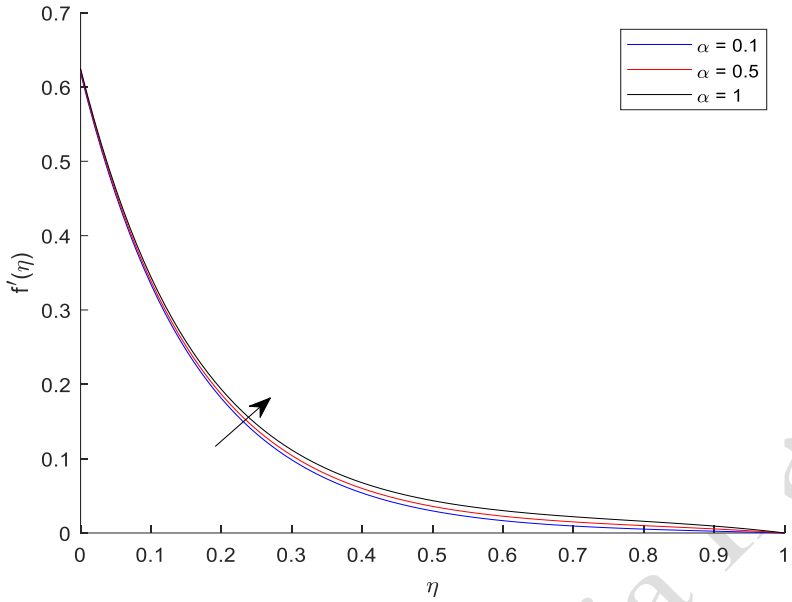

Fig. 3. $f'(\eta)$ Profile for different values of α

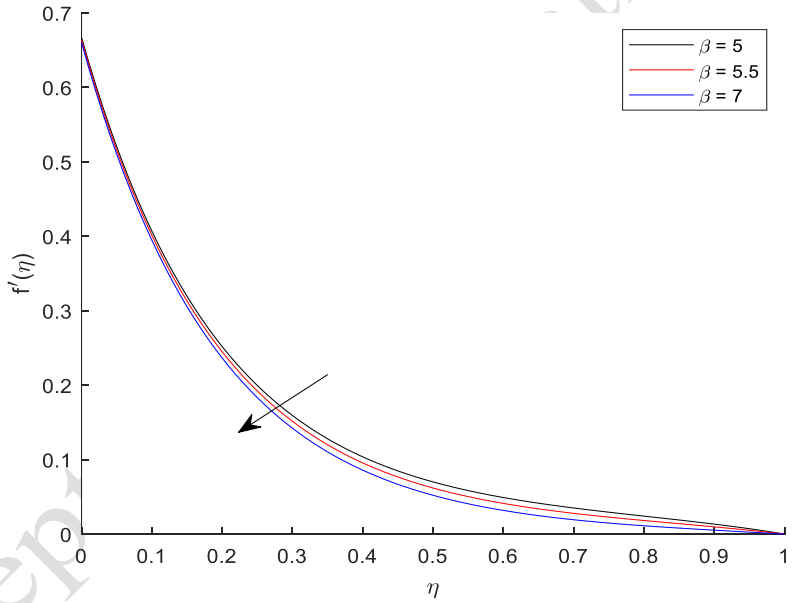

Fig. 4. $f'(\eta)$ Profile for different values of β

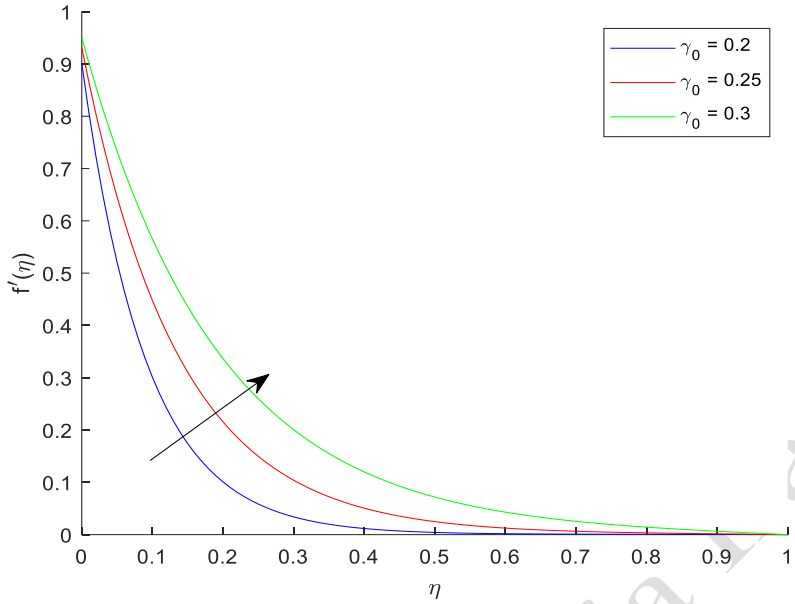

Fig. 5. $f'(\eta)$ Profile for different values of γ_0

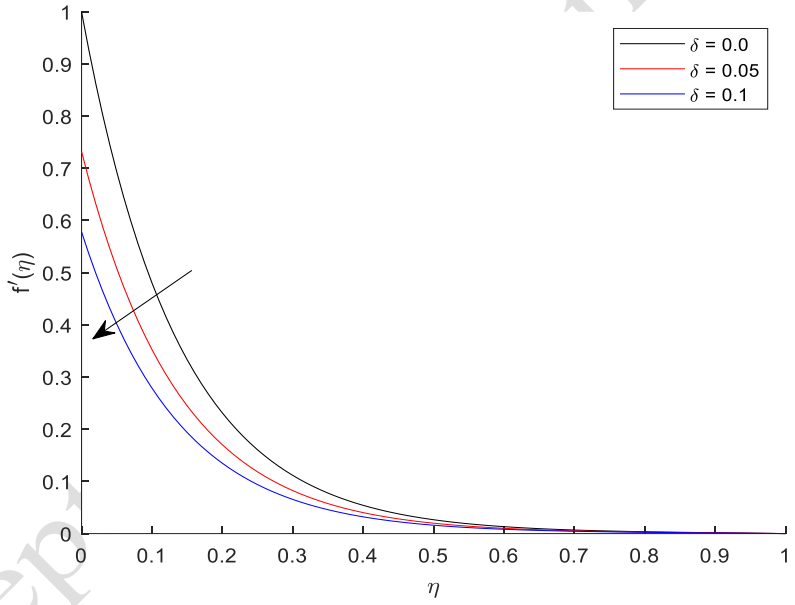

Fig. 6. $f'(\eta)$ Profile for different values of δ

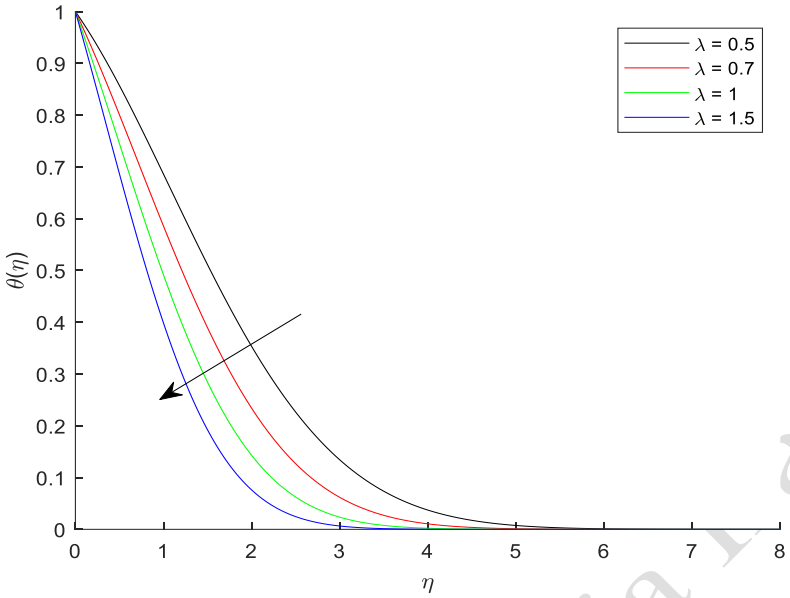

Fig. 7. $\theta(\eta)$ Profile for different values of λ

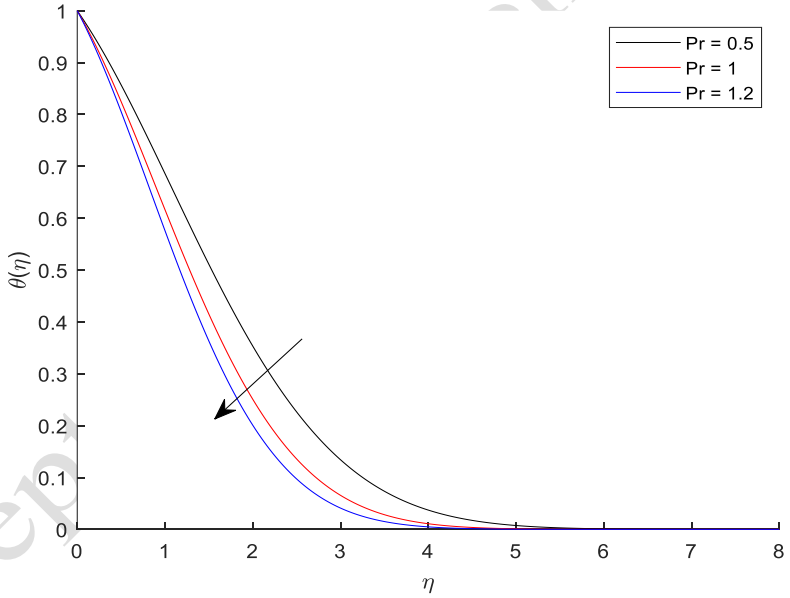

Fig. 8. $\theta(\eta)$ Profile for different values of Pr

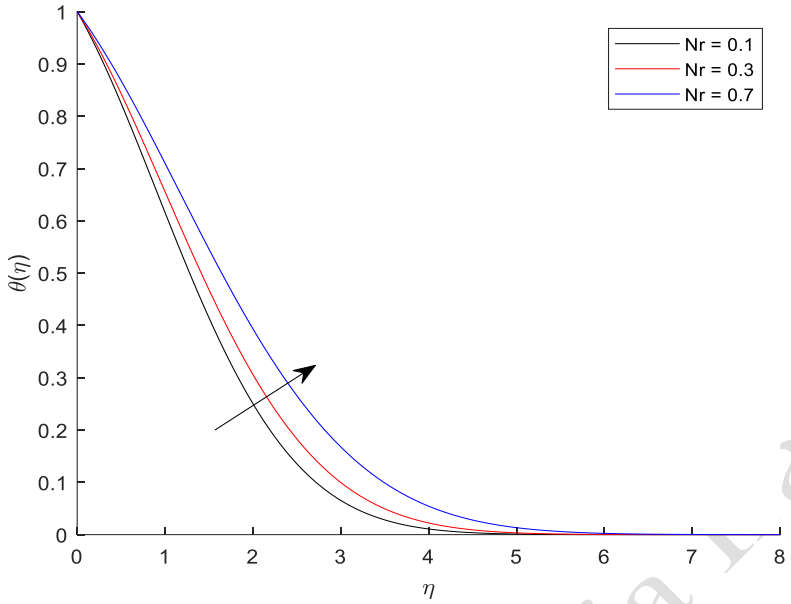

Fig. 9. $\theta(\eta)$ Profile for different values of Nr

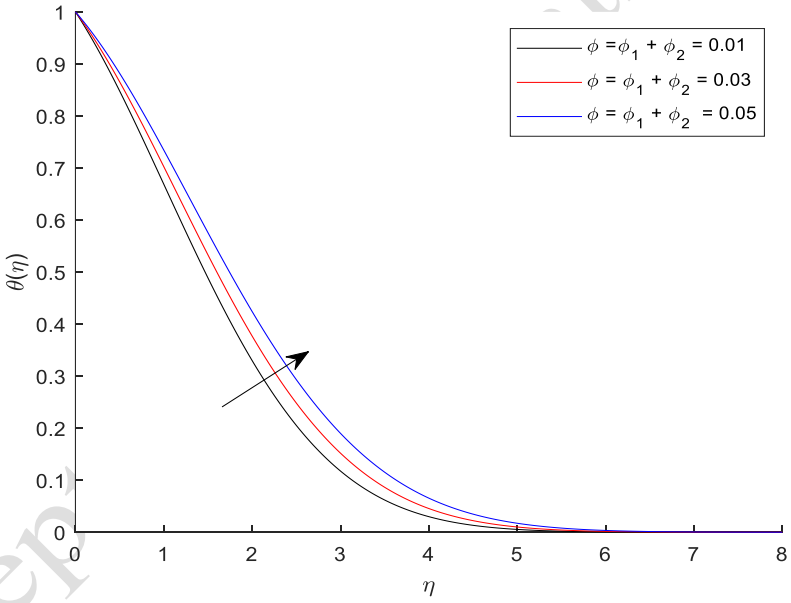

Fig. 10. $\theta(\eta)$ Profile for different values of ϕ

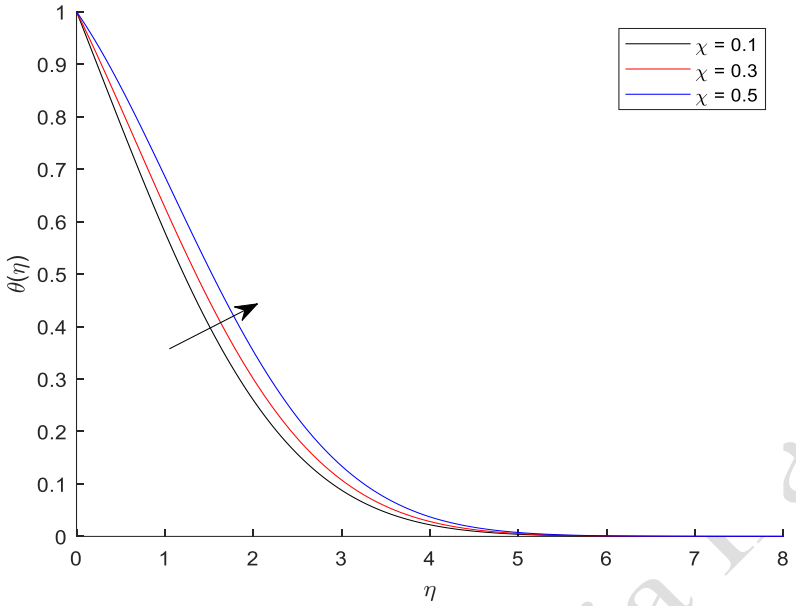

Fig. 11. $\theta(\eta)$ Profile for different values of χ

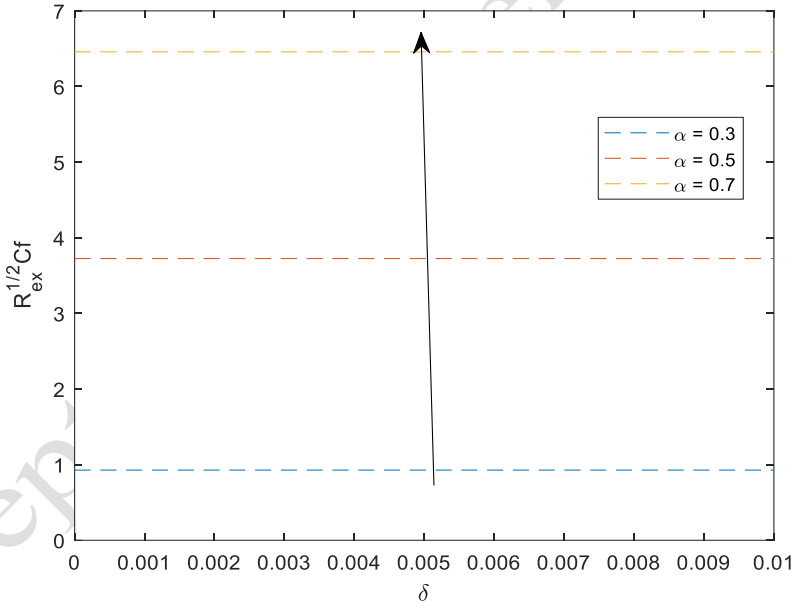

Fig. 12. $\mathrm{Re}_x^{1/2} C_f$ variations with δ for different values of α

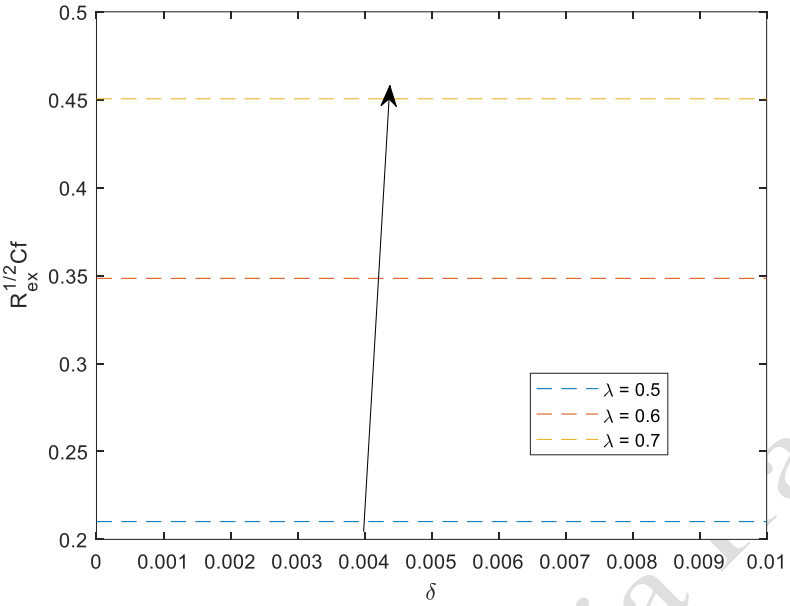

Fig. 13. $\mathrm{Re}_x^{1/2} C_f$ variations with δ for different values of λ

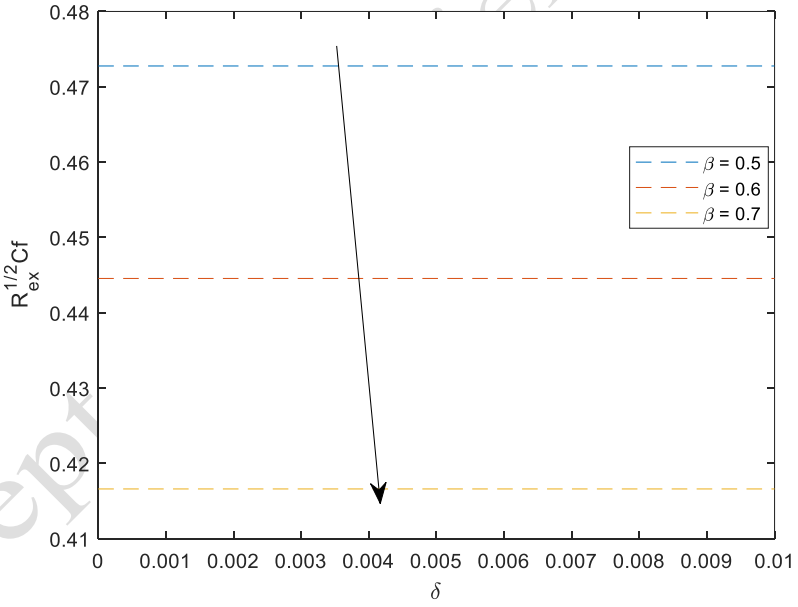

Fig. 14. $\mathrm{Re}_x^{1/2} C_f$ variations with δ for different values of β

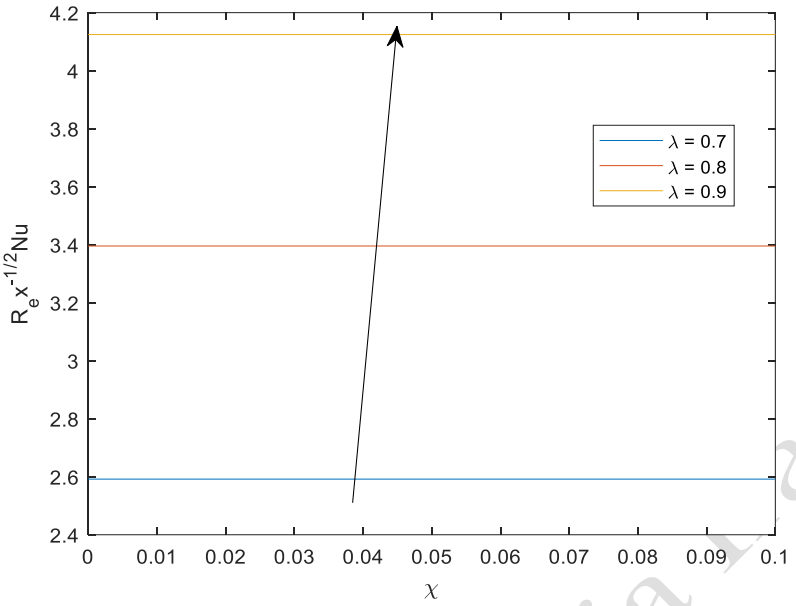

Fig. 15. $\mathrm{Re}_x^{-1/2}\, Nu_x$ variations with χ for different values of λ

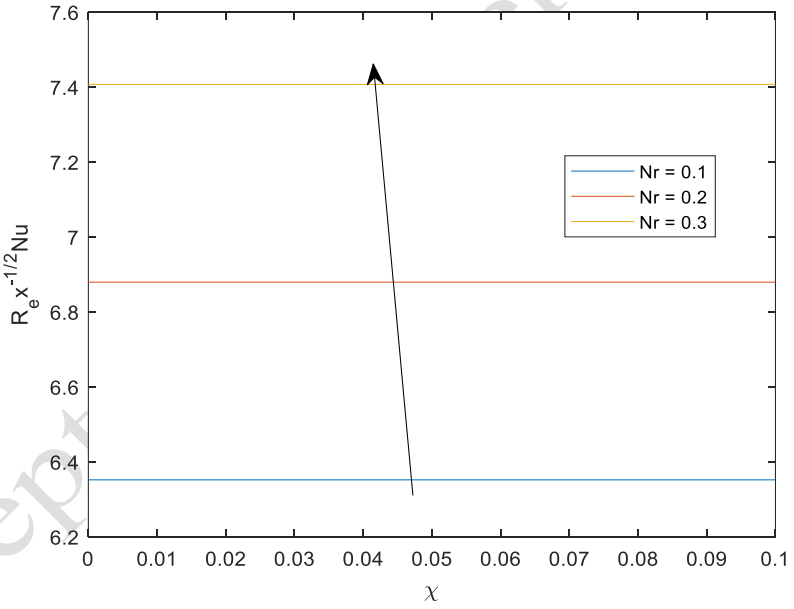

Fig. 16. $\mathrm{Re}_x^{-1/2}\, Nu_x$ variations with χ for different values of Nr

Table 1. The thermal relations for hybrid nanomaterials [28-29]

Property	Hybrid nanomaterial
Absolute viscosity	$\mu_{hnf} = \mu_f \left\{ (1-\phi_1)^{-2.5} (1-\phi_2)^{-2.5} \right\}$
Density	$\rho_{hnf} = \rho_f \left((1-\phi_2) \left[(1-\phi_1) + \phi_1 \frac{\rho_{s1}}{\rho_f} \right] + \phi_2 \frac{\rho_{s2}}{\rho_f} \right)$
Heat capacity	$\left(\rho c_p\right)_{hnf} = \left(\rho c_p\right)_f \left((1-\phi_2) \left[(1-\phi_1) + \phi_1 \frac{\left(\rho c_p\right)_{s1}}{\left(\rho c_p\right)_f} \right] + \phi_2 \frac{\left(\rho c_p\right)_{s2}}{\left(\rho c_p\right)_f} \right)$
Thermal conductivity	$\left.\begin{aligned} \frac{k_{hnf}}{k_{nf}} &= \frac{(1-\phi_2) + 2\phi_2 \left(\frac{k_{s2}}{k_{s2}-k_{nf}} \right) ln\left(\frac{k_{s2}+k_{nf}}{k_{nf}} \right)}{(1-\phi_2) + 2\phi_2 \left(\frac{k_{nf}}{k_{s2}-k_{nf}} \right) ln\left(\frac{k_{s2}+k_{nf}}{k_{nf}} \right)} \\ \frac{k_{hnf}}{k_{nf}} &= \frac{(1-\phi_2) + 2\phi_2 \left(\frac{k_{s2}}{k_{s2}-k_{nf}} \right) ln\left(\frac{k_{s2}+k_{nf}}{k_{nf}} \right)}{(1-\phi_2) + 2\phi_2 \left(\frac{k_{nf}}{k_{s2}-k_{nf}} \right) ln\left(\frac{k_{s2}+k_{nf}}{k_{nf}} \right)} \end{aligned}\right\}$
Electrical conductivity	$\left.\begin{aligned} \frac{\sigma_{hnf}}{\sigma_{nf}} &= \frac{\sigma_{s2} + 2\sigma_{nf} - 2\phi_2 \left(\sigma_{nf} - \sigma_{s2} \right)}{\sigma_{s2} + 2\sigma_{nf} + \phi_2 \left(\sigma_{nf} - \sigma_{s2} \right)} \\ \frac{\sigma_{nf}}{\sigma_f} &= \frac{\sigma_{s1} + 2\sigma_f - 2\phi_1 \left(\sigma_f - \sigma_{s1} \right)}{\sigma_{s1} + 2\sigma_f + \phi_1 \left(\sigma_f - \sigma_{s1} \right)} \end{aligned}\right\}$

Table 2. Thermal features of the base and nanoparticles

	$\rho\left(kg/m^3\right)$	$C_p\left(J/kgK\right)$	$k\left(W/mK\right)$	$\sigma\left(\Omega m\right)^{-1}$
Pure water (H_2O)	997.1	4179	0.613	0.05
AA7072	x2720	893	222	34.83×10^6
AA7075	2810	960	173	26.7710^6

Table 3. Comparison of present result for varied values of α and χ

α	χ	Present result $\mathrm{Re}_x^{1/2} C_f$	Khan et al. [38] $\mathrm{Re}_x^{1/2} C_f$
0.1	0.1	0.224565	0.22432671582
0.3	0.3	0.242737	0.242652782431
0.7	0.7	0.263675	0.263526178920
0.9	0.9	0.287147	0.287325617829

Dr. Satya Ranjan Mishra currently working as Professor, Department of Mathematics, Siksha O Anusandhan Deemed to be University, Bhubaneswar. He has 21 years of teaching experience in both PG and UG level. He did his Ph.D. from Siksha O Anusandhan in 2013 and since then actively engaged in his research work. His area of interest is Heat transfer, Magnetohydrodynamics, Porous media, etc. with the broad area of Fluid Dynamics. He has published nearly **410 papers** in the international journals of repute and all are either SCI or Scopus indexed that can be viewed in various databases like Scopus, Research gate, Google scholar, etc. With a huge citation of his work, he took a position of **Top 2% World Scientists by Stanford University, USA** in 5 consecutive years i.e., 2020-2024. He has also **guided 15 research scholars** and six more students are working under his guidance. Dr. Mishra Delivered several lectures in various conferences and Faculty development program organized by Rajasthan Technical University, Rajasthan in 2019 on the topic "Introduction to MATLAB", FDP organized by Poornima Group of Institutions, Rajasthan on the topic "Numerical solutions using scientific tool MAPLE" in 2020 (online), Summer instructional School organized by NIT Arunachachal Pradesh on the topic "Linear Algebra" in the year 2020. As strength he has **edited a book series in Springer Nature** for the year 2020 as a leading Editor and also Editor/associate editor in several reputed international journals. Dr. Mishra wrote a Book entitled "Learning Numerical Method using MATLAB" under the Bentham Science publisher, UAE and going to be publish soon in this year.

Dr. MD. Shamshuddin has completed his Masters in Mathematics from Osmania University in the year 2002; and also completed his M. Phil from Sri Venkateswara University in the year 2010. He received his prestigious PhD degree in Applied Mathematics at GITAM Deemed to be

University, Andhra Pradesh in the year 2019. He has published more than **210 International repute articles** through various journals and Conferences of repute and all are either SCI or Scopus indexed that can be viewed in various databases like Scopus, Research gate, Google scholar, etc. With a huge citation of his work, he took a position of **Top 2% World Scientists by Stanford University, USA in the year 2023 and 2024**. Currently, his research interest is in fluid mechanics, magnetofluid dynamics, micropolar fluid, nanofluid and hybrid nanofluids and heat and mass transfer, solar radiation, energy, with its applications. He is a seasoned researcher with strong mentality and sound analytical mind, and he has contributed tremendously in his core areas of research. He has reviewed several research articles for many journals and publishers.

Dr. Subhajit Panda currently working as Assistant Professor, Centre for Data Science, Department of Computer Science and Engineering, Siksha O Anusandhan Deemed to be University, Bhubaneswar. He did his Ph.D. from NIT Mizoram in 2025 and since then actively engaged in his research work. His area of interest is Heat transfer, Magnetohydrodynamics, Porous media, etc. with the broad area of Fluid Dynamics. He has published nearly **107 papers** in the international journals of repute and all are either SCI or Scopus indexed that can be viewed in various databases like Scopus, Research gate, Google scholar, etc.

Prof. Wubshet Ibrahim

Prof. Wubshet Ibrahim completed his Master's degree in Mathematics from Addis Ababa University, Ethiopia, in 2005, and earned his PhD in Applied Mathematics from Osmania University, Hyderabad, India, in 2013. He has published over **100 research** articles in reputable international journals all indexed in Web of Science or Scopus. Currently, his research interests include fluid mechanics, magnetofluid dynamics, micropolar fluids, nanofluids and hybrid nanofluids, heat and mass transfer, and energy-related applications. Prof. Wubshet is a seasoned researcher with a strong analytical mindset and a deep commitment to advancing scientific knowledge. He has served as a reviewer for numerous prestigious journals and publishers. In addition, he has supervised several PhD students in the field of nanofluid dynamics and has acted as an external examiner for many doctoral dissertations in fluid dynamics. His contributions to the field have had a significant impact on both academic research and practical applications.

Rupa Baithalu has completed his Masters in Mathematics from Siksha O Anusandhan University in the year 2022. Now she has currently continuing as a Research scholar, Department of Mathematics, Siksha O Anusandhan Deemed to be University, Bhubaneswar. Her area of interest is Heat transfer, Magnetohydrodynamics, Porous media, etc. with the broad area of Fluid Dynamics. He has published nearly **56 papers** in the international journals of repute and all are either SCI or Scopus indexed that can be viewed in various databases like Scopus, Research gate, Google scholar, etc.